Backbone Dynamics of Alamethicin Bound to Lipid Membranes: Spin-Echo Electron Paramagnetic Resonance of TOAC-Spin Labels

Rosa Bartucci,* Rita Guzzi,* Marta De Zotti,† Claudio Toniolo,† Luigi Sportelli,* and Derek Marsh‡
*Dipartimento di Fisica, Università della Calabria, 87036 Arcavacata di Rende (CS), Italy; †Institute of Biomolecular Chemistry, Padova Unit, Consiglio Nazionale delle Ricerche, Department of Chemistry, University of Padova, 35131 Padova, Italy; and ‡Max-Planck-Institut für biophysikalische Chemie, Abt. Spektroskopie, 37077 Göttingen, Germany

ABSTRACT Alamethicin F50/5 is a hydrophobic peptide that is devoid of charged residues and that induces voltage-dependent ion channels in lipid membranes. The peptide backbone is likely to be involved in the ion conduction pathway. Electron spin-echo spectroscopy of alamethicin F50/5 analogs in which a selected Aib residue (at position $n = 1$, 8, or 16) is replaced by the TOAC amino-acid spin label was used to study torsional dynamics of the peptide backbone in association with phosphatidylcholine bilayer membranes. Rapid librational motions of limited angular amplitude were observed at each of the three TOAC sites by recording echo-detected spectra as a function of echo delay time, 2τ. Simulation of the time-resolved spectra, combined with conventional EPR measurements of the librational amplitude, shows that torsional fluctuations of the peptide backbone take place on the subnanosecond to nanosecond timescale, with little temperature dependence. Associated fluctuations in polar fields from the peptide could facilitate ion permeation.

INTRODUCTION

Alamethicin is a 19-amino acid residue, hydrophobic peptide from the microorganism *Trichoderma viride*; it is extended at the C-terminus by the 1,2-amino alcohol phenylalaninol and is blocked at the N-terminus by an acetyl group. This peptaibol contains a preponderance of the C^{α}-tetrasubstituted α-amino acid Aib and is helical in conformation with a bend near the internal proline residue, Pro^{14} (1). In lipid membranes, alamethicin induces transient voltage-dependent ion channels that undergo step-like transitions between different conductance states. The characteristics of these peptide-induced ion channels are dependent on the properties of the lipid membrane environment (2–5).

Various spectroscopic studies indicate that, in the absence of a transmembrane potential, the alamethicin peptide is predominantly monomeric in lipid bilayer membranes, if these are in the physiologically relevant fluid state (6–9). This finding is in agreement with mechanistic studies, which reveal that initiation of channel conductance is a highly cooperative process and suggest that transitions between different conductance levels take place by incorporation of alamethicin monomers into preexisting pore aggregates (10).

Investigations on the orientation and mode of incorporation of alamethicin in phospholipid bilayer membranes have been aided recently by the use of TOAC spin labels that are incorporated at selected positions in the peptide backbone (8,9). TOAC is a nitroxyl α-amino acid that can serve as an EPR-active reporter of peptide location and dynamics (11–16). Because TOAC is a helicogenic, C^{α}-tetrasubstituted α-amino acid it provides a conservative substitution for Aib residues at different positions in the sequence of alamethicin. Electrophysiological experiments show that the TOAC-substituted analogs are functionally active, and crystal-structure determination reveals a helical conformation that is closely similar to that of native alamethicin (17).

In previous work, we determined the orientational ordering and overall rotational dynamics of TOAC-labeled alamethicin by using CW-EPR methods (8,9). The latter studies refer to rotational diffusion around the peptide axis of alamethicin and to off-axis angular excursions of the peptide backbone about the membrane normal. These motional modes are relevant to oligomeric assembly and pore formation but do not refer specifically to torsional flexing of the peptide backbone, which could be a significant component of the ion transport process (18–20).

In this work, we use time-resolved EPR to study torsional librations in the backbone of TOAC-labeled alamethicin by means of electron spin-echo spectroscopy (see, e.g., Bartucci et al. (21)). This method was used already to characterize the librational motion of spin-labeled lipid chains in phospholipid bilayer membranes (22–24) and in the fatty acid binding site of serum albumin (25). ED-spectra as a function of interpulse delay time yield values for the product of the mean-square torsional amplitude, $\langle\alpha^2\rangle$, and the librational correlation time, τ_c. Complementary CW-EPR measurements give the torsional amplitude and, hence (from the ED-spectra),

Submitted June 15, 2007, and accepted for publication November 29, 2007.

Address reprint requests to Derek Marsh, Tel.: +49-551-201-1285; Fax: +49-551-201-1501; E-mail: dmarsh@gwdg.de.

Abbreviations used: Aib, α-aminoisobutyric acid; CW, continuous wave; DMPC, 1,2-dimyristoyl-*sn*-glycero-3-phosphocholine; ED, echo-detected; EPR, electron paramagnetic resonance; FT, Fourier transform; Phol, phenylalaninol; TEMPOL, 4-hydroxy-2,2,6,6-tetramethylpiperidine-1-oxyl; TOAC, 2,2,6,6-tetramethylpiperidine-1-oxy-4-amino-4-carboxylic acid; $TOAC^{n}$-Alm, $[Glu(OMe)^{7,18,19}]$-alamethicin F50/5 with TOAC substituted at residue position *n*.

Editor: Anthony Watts.

0006-3495/08/04/2698/08 $2.00

doi: 10.1529/biophysj.107.115287

the correlation time, τ_c. Typically, the latter corresponds to the subnanosecond to nanosecond regime of rapid, small-amplitude, oscillatory motions that could effect time-dependent electric field fluctuations and dielectric relaxation.

MATERIALS AND METHODS

Materials

DMPC was from Sigma-Aldrich (St. Louis, MO). Spin-labeled analogs of alamethicin F50/5 [TOAC^n, Glu(OMe)^{7,18,19}] with $n = 1$, 8, or 16 (where Glu(OMe) is γ-methyl glutamic acid, replacing a Gln residue in the natural sequence) were synthesized according to Peggion et al. (26,27). The complete amino acid sequences of the three TOAC^n-Alm derivatives are:

Ac-TOAC-Pro-Aib-Ala-Aib-Ala-Glu(OMe)-Aib-Val-Aib-Gly-Leu-Aib-Pro-Val-Aib-Aib-Glu(OMe)-Glu(OMe)-Phol [TOAC^1,Glu(OMe)^{7,18,19}]
Ac-Aib-Pro-Aib-Ala-Aib-Ala-Glu(OMe)-TOAC-Val-Aib-Gly-Leu-Aib-Pro-Val-Aib-Aib-Glu(OMe)-Glu(OMe)-Phol [TOAC^8,Glu(OMe)^{7,18,19}]
Ac-Aib-Pro-Aib-Ala-Aib-Ala-Glu(OMe)-Aib-Val-Aib-Gly-Leu-Aib-Pro-Val-TOAC-Aib-Glu(OMe)-Glu(OMe)-Phol [TOAC^{16},Glu(OMe)^{7,18,19}]

Circular dichroism in MeOH shows that all three analogs are folded in similar, highly helical conformations (28). CW-EPR additionally shows that the analogs are monomeric in MeOH (15).

Sample preparation

DMPC and 1 mol % of the desired TOAC spin-labeled alamethicin (in MeOH) were codissolved in $CHCl_3$, and the solution was then evaporated with dry nitrogen. After keeping it under vacuum overnight, the dry mixture was dispersed in water at a concentration of ~100 mg/ml by vortex mixing while heating to above the chain-melting transition of DMPC. The hydrated lipid bilayers were transferred to a standard 4-mm-diameter quartz EPR tube, concentrated by pelleting in a benchtop centrifuge, and the excess water was removed.

EPR spectroscopy

Pulsed EPR data were collected on an ELEXSYS E580 9-GHz FT-EPR spectrometer (Bruker, Karlsruhe, Germany) equipped with a MD5 dielectric resonator and a CF 935P cryostat (Oxford Instruments, Abingdon, UK). Two-pulse ($\pi/2$ - τ - π - τ - echo) ED-EPR spectra were obtained by recording the integrated spin-echo signal at fixed interpulse delay τ while sweeping the magnetic field. The integration window was 160 ns. The microwave pulse widths were 32 ns and 64 ns, with the microwave power adjusted to provide $\pi/2$ and π-pulses, respectively.

The original ED-spectra, $ED_T(2\tau,B)$, were corrected for instantaneous spin diffusion by normalizing with respect to those recorded at 77 K, where no molecular motion is expected. The corrected spectra, $ED_T^{corr}(2\tau,B)$, recorded at temperature T are plotted as a function of magnetic field B according to (23)

$$ED_T^{corr}(2\tau,B) = ED_T(2\tau,B)\frac{ED_{77K}(2\tau_0,B)}{ED_{77K}(2\tau,B)}, \quad (1)$$

where τ_0 is the shortest value of τ for which ED-spectra were obtained. Relaxation rates, $W(B,\tau_1,\tau_2)$, were determined from the ratio of corrected ED-spectra recorded at two different values, τ_1 and τ_2, of the interpulse delay by using the following relation (24):

$$W(B,\tau_1,\tau_2) = \ln\left[\frac{ED(2\tau_1,B)}{ED(2\tau_2,B)}\right] \times \frac{1}{2(\tau_2-\tau_1)}, \quad (2)$$

where $ED(2\tau,B)$ is the ED-spectral line height at field position B. These relaxation rates are averaged over the time interval from τ_1 to τ_2 and are characterized by the maximum values, W_L and W_H, determined in the low- and high-field regions, respectively, of the ED-spectra. At least two interpulse delay times are required to determine the relaxation rate. For an exponential echo decay (22), the relaxation rate is independent of the choice of τ_1 and τ_2 (23); in practice, the pair of delay times is chosen to give the best signal/noise ratio in the values of W (see Fig. 2 *b*). Calibration of the W_L and W_H relaxation rates in terms of the amplitude-correlation time product, $\langle\alpha^2\rangle\tau_c$, of rotational motion from low-amplitude librations is taken from the results of spectral simulations (see below). Here, α is the angular amplitude, τ_c is the correlation time, and angular brackets indicate an average over the librational motion.

ED-spectra were simulated by using the so-called ''isotropic'' librational model described in Erilov et al. (23,24). In this model, simultaneous independent (i.e., uncorrelated) librational motions take place around three mutually perpendicular axes: x, y, and z. In the fast motional limit, i.e., $\langle\Delta\omega^2\rangle\tau_c^2 \ll 1$, the decay of the echo amplitude is given by (23)

$$ED(2\tau,B) \approx \exp\left(-2\langle\Delta\omega^2(B)\rangle\tau_c\tau\right), \quad (3)$$

where $\langle\Delta\omega^2(B)\rangle$ is the mean-square fluctuation in angular resonance frequency, which is proportional to $\langle\alpha^2\rangle$, the mean-square amplitude of libration. For instance, the shift in angular resonance frequency caused by a libration of small amplitude, α, about the nitroxide x axis is (29)

$$\Delta\omega(\theta,\varphi) = \alpha\left[\frac{\beta}{\hbar}B(g_{yy}-g_{zz}) + \frac{m_I(A_{yy}^2-A_{zz}^2)}{\sqrt{(A_{xx}^2\cos^2\varphi + A_{yy}^2\sin^2\varphi)\sin^2\theta + A_{zz}^2\cos^2\theta}}\right]\sin\theta\cos\theta\sin\varphi, \quad (4)$$

where m_I is the ^{14}N-nuclear magnetic quantum number, and θ, ϕ are polar coordinates of the magnetic field direction in the molecular frame. The isotropic model, in contrast to uniaxial libration, reduces the dependence on the magnetic field orientation (θ,ϕ) and ensures that the echo decay is approximately exponential, as indicated by Eq. 3. In this model, the relaxation rate defined by Eq. 2 is given by $W(B) = \langle\Delta\omega^2(B)\rangle\tau_c$ and is independent of the values of τ_1 and τ_2. Instantaneous diffusion that arises from spin-spin interactions between nitroxides (30) is also included in the simulations (23).

Spin-Hamiltonian parameters were determined—simultaneously with the librational amplitude-correlation time product, $\langle\alpha^2\rangle\tau_c$, and the instantaneous diffusion—by simulation of the ED-spectra recorded at 200 K. These three sets of parameters have distinctly different effects on the ED-line shapes as a function of the echo delay time, τ. For TOAC^{16}-Alm, the effective spin-Hamiltonian parameters determined in this way were $A_{xx} = 5.2$ G, $A_{yy} = 3.5$ G, $A_{zz} = 32.3$ G and $g_{xx} = 2.0093$, $g_{yy} = 2.0064$, $g_{zz} = 2.0024$. These values change somewhat for the other spin-label positions because of the different environmental polarities (8) and possibly also because of slight differences in conformation of the TOAC ring (cf. Marsh (31)). The values of A_{zz} (and g_{zz}) agree with those determined from rigid-limit CW-EPR spectra. For com-

parison with the effective spin-Hamiltonian parameters for TOAC, the tensors of TEMPOL determined in a single-crystal host are $A_{xx} = 5.3$ G, $A_{yy} = 7.0$ G, $A_{zz} = 35.0$ G and $g_{xx} = 2.0099$, $g_{yy} = 2.0061$, $g_{zz} = 2.0024$ (32). The low effective value of A_{yy} is a particular feature of the isotropic librational model when used to describe the ED-spectra as a function of τ. This has been found previously when using the same isotropic librational model to simulate the ED-spectra of spin-labeled lipid chains (23,24). Evidently, this modification of the tensor values is necessary to enable the simple isotropic model to describe the effects of librational dynamics adequately. ED-spectra recorded at other temperatures, both above and below 200 K, were then simulated with fixed effective tensor values, principally by changing the librational amplitude-correlation time product, $\langle\alpha^2\rangle\tau_c$, but also by adjusting the parameter for the instantaneous diffusion.

Conventional CW-EPR spectra were recorded on an ESP-300 9-GHz spectrometer (Bruker) using 100-kHz field modulation; the spectrometer was equipped with an ER 4111VT temperature controller.

RESULTS

ED-EPR spectra and simulations

Fig. 1 shows the ED-EPR spectra of the TOAC residue substituted at sequence position 1, 8, or 16 in [Glu(OMe)^{7,18,19}]-alamethicin (TOAC^1-, TOAC^8-, or TOAC^{16}-Alm, respectively). Spin-labeled alamethicin is incorporated in DMPC bilayer membranes and the spectra are recorded at 200 K. The solid lines in Fig. 1 are original experimental spectra after correction for instantaneous diffusion according to Eq. 1 with $\tau_0 =$ 168 ns, by using spectra additionally recorded at 77 K. The dependence of the ED-line shapes on the echo delay time, τ, is characteristic of small-amplitude torsional librations, as is seen from the preferential decay in the intermediate spectral regions at low and high field with increasing delay time, τ (see, e.g., Dzuba et al. (29) and Dzuba (33)). The dynamic parameter that determines the influence of the librational motion on the shape of the ED-spectra at nonzero τ is the product of the mean-square torsional amplitude, $\langle\alpha^2\rangle$, and the librational correlation time, τ_c.

ED-spectra simulated by using the isotropic librational model (i.e., independent librations about three perpendicular axes) are given by the dashed lines in Fig. 1 (see Materials and Methods for details). These simulations include the effects of instantaneous diffusion on the ED-line shapes in the time interval before the first echo delay time, $\tau_0 = 168$ ns. (The experimental spectra are already corrected for instantaneous diffusion occurring after this time by using Eq. 1.) As seen in Fig. 1, the dependence of the corrected experimental spectra on echo delay time is described adequately by these simulations for all three positions of TOAC. The degree of agreement between simulated and experimental spectra is comparable to that achieved previously for the ED-spectra of spin-labeled lipid chains when using the same isotropic librational model (23). Amplitude-correlation time products, $\langle\alpha^2\rangle\tau_c$, for the librational motions that are deduced from the spectral simulations in Fig. 1, *a–c*, exhibit quantitative differences (which are implicit in the slightly different ED-line shapes for the three TOAC positions) but are of a similar order of magnitude. The level of instantaneous diffusion differs somewhat between the different TOAC positions but also depends to some extent on the sample preparation conditions. ED-spectra recorded at higher temperatures can then be consistently simulated solely by increasing the amplitude-correlation time product for the librational motion (and decreasing the extent of instantaneous diffusion).

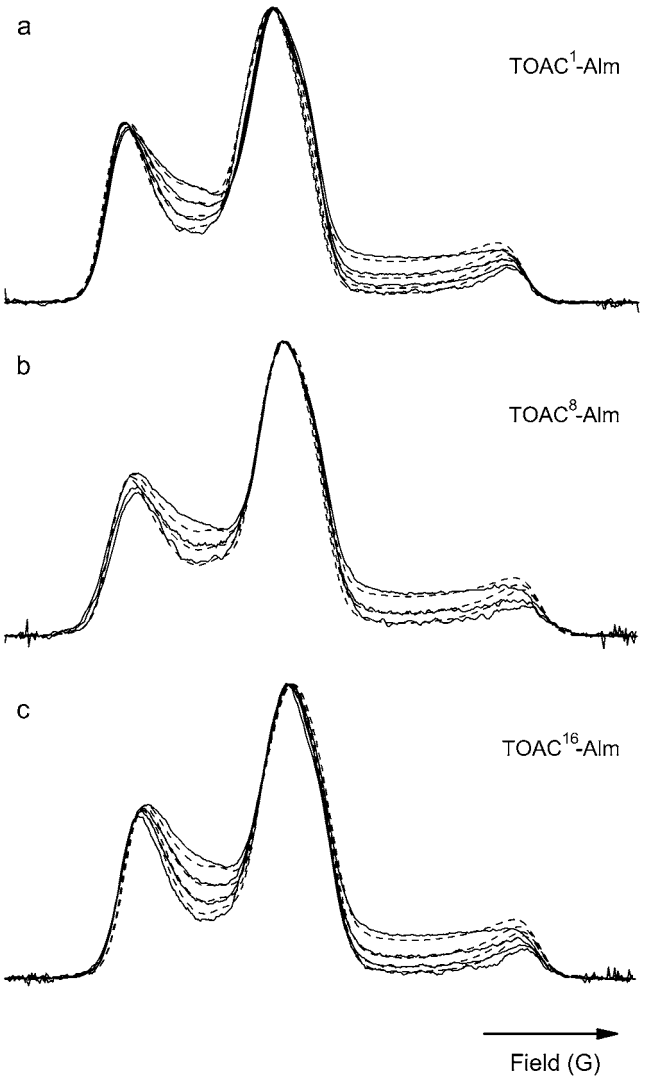

FIGURE 1 ED-EPR spectra of [Glu(OMe)^{7,18,19}]-alamethicin with TOAC substituted for (*a*) residue 1 (TOAC^1-Alm), (*b*) residue 8 (TOAC^8-Alm), and (*c*) residue 16 (TOAC^{16}-Alm) in DMPC bilayers at $T = 200$ K. ED-spectra are recorded for increasing interpulse spacings of (*top* to *bottom*) $\tau = 168$, 296, 424, and 552 ns and are normalized to the maximum line height. Total scan width is 100 G. Solid lines are the original experimental spectra with correction for instantaneous diffusion according to Eq. 1, and dashed lines are simulations for isotropic librational motion including the effects of instantaneous diffusion for the first-recorded spectrum at $\tau = 168$ ns (see text). The amplitude-correlation time products used in the simulations are $\langle\alpha^2\rangle\tau_c = 6.5$, 6.0, and 7.5×10^{-12} rad^2 s for TOAC^1-Alm, TOAC^8-Alm, and TOAC^{16}-Alm, respectively.

ED-relaxation spectra and hyperfine splittings

Fig. 2 shows an alternative means of analyzing the ED-spectra by using the *W*-relaxation parameter (24). This method has the advantage that it reflects systematic changes in experimental parameters, e.g., temperature variation, directly. ED-spectra of TOAC^{16}-Alm—recorded at 200 K and corrected for instantaneous diffusion according to Eq. 1 by using spectra additionally recorded at 77 K—are given for reference in Fig. 2 *a*. Corresponding spectral plots of the *W*-relaxation parameter for TOAC^{16}-Alm—evaluated from two pairs of corrected ED-spectra with different combinations of the echo delay times, τ_1 and τ_2, according to Eq. 2—are given in Fig. 2 *b*. *W*-relaxation curves that are evaluated for different pairs of τ_1 and τ_2 coincide to within the noise level, showing that the relaxation is close to exponential (cf. Eq. 3). The latter feature is consistent with the isotropic model for librational dynamics but not with those for uniaxial libration (23). The spectral simulations that were given above allow calibration of the *W*-relaxation parameter in terms of the amplitude-correlation time product for isotropic libration (see below).

Fig. 3 *a* shows the temperature dependence of the maximum values, W_L and W_H, of the ED-EPR relaxation rates in the low- and high-field regions for the TOAC^n-Alm derivatives in DMPC bilayers. The temperature profiles of W_L (*solid symbols*) and W_H (*open symbols*) are very similar, showing consistency between the low- and high-field regions of the ED-spectra. The two profiles can be brought into numerical accord by multiplying the absolute values of W_L by a factor of ~2.5–2.9× for TOAC^8 and TOAC^{16} and of 3.1–3.3× for TOAC^1. Simulations for librational motion of a doxyl spin label (14-doxyl phosphatidylcholine) predict a similar conversion factor of 2.8× between W_L and W_H (24). It is seen from Fig. 3 *a* that the intensity of librational motion (i.e., the value of the amplitude-correlation time product, $\langle\alpha^2\rangle\tau_c$) increases relatively slowly from 77 K to 180 K and then more steeply beyond this temperature. The values of W_L and W_H are rather similar for the TOAC^8 and TOAC^{16} positions, whereas those for the TOAC^1 position at the higher temperatures are definitely larger.

Fig. 3 *b* shows the dependence of the outer hyperfine splitting, $2\langle A_{zz}\rangle$, in the conventional CW-EPR spectra on

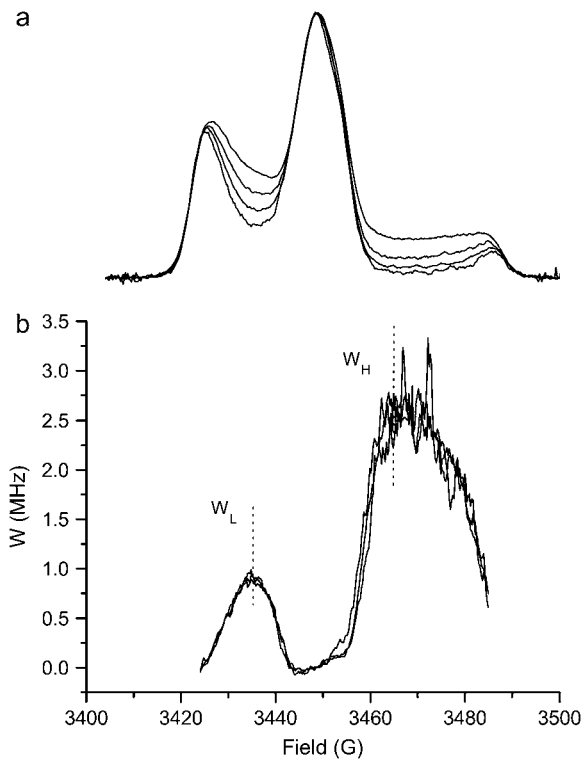

FIGURE 2 (*a*) Corrected ED-EPR spectra of TOAC^{16}-Alm in DMPC bilayers at $T = 200$ K. ED-spectra are recorded for interpulse spacings of (*top* to *bottom*) $\tau = 168$, 296, 424, and 552 ns. Spectra are corrected for instantaneous spin diffusion according to Eq. 1 and are normalized to the maximum line height. (*b*) Anisotropic part of the relaxation rate, *W*, obtained according to Eq. 2 from pairs of spectra in (*a*) with interpulse separations of $\tau_1 = 168$ and $\tau_2 = 296$ ns, $\tau_1 = 168$ and $\tau_2 = 424$ ns, or $\tau_1 = 168$ and $\tau_2 = 552$ ns.

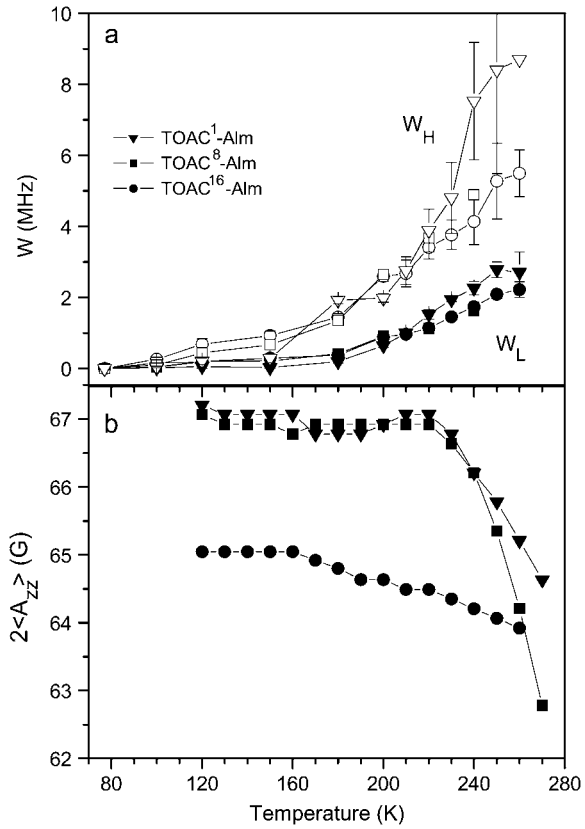

FIGURE 3 (*a*) Temperature dependence of the W_L (*solid symbols*) and W_H (*open symbols*) ED-EPR relaxation rate parameters for TOAC^n-Alm ($n = 1$, 8, or 16) in DMPC bilayers. Determinations of *W* are for $\tau_1 = 168$ ns and $\tau_2 = 296$ ns (see Eq. 2). (*b*) Temperature dependence of the outer hyperfine splitting, $2\langle A_{zz}\rangle$, in the conventional CW-EPR spectra of TOAC^n-Alm ($n = 1$, 8, or 16) in DMPC bilayers.

temperature for the TOAC^n-Alm derivatives in DMPC bilayers. For small-amplitude fast librations, the partially averaged hyperfine splitting, $\langle A_{zz}\rangle$, is related directly to the mean-square torsional amplitude, $\langle\alpha^2\rangle$ (34). The values of $\langle A_{zz}\rangle$ for TOAC^1- and TOAC^8-Alm in DMPC bilayers remain rather constant up to ~220 K. Beyond this, $\langle A_{zz}\rangle$ decreases progressively with increasing temperature for both TOAC^1- and TOAC^8-Alm, corresponding to increasing amplitudes of torsional libration. The rate of change with increasing temperature is greater for TOAC^8-Alm than for TOAC^1-Alm. For TOAC^{16}-Alm, the values of $\langle A_{zz}\rangle$ remain constant only up until ~160 K; at this residue position, librational motion sets in at a lower temperature than for TOAC^1- and TOAC^8-Alm but increases in amplitude rather slowly with increasing temperature.

Characterization of librational motion

Fig. 4 *a* shows the temperature dependence of the librational amplitude-correlation time product, $\langle\alpha^2\rangle\tau_c$, for the TOAC^n-Alm derivatives in DMPC bilayers. These values are obtained from the measurements of W_L that are given in Fig. 3 *a*, together with the simulations for isotropic libration at 200 K that are given in Fig. 1. The conversion factor relating $\langle\alpha^2\rangle\tau_c$ to W_L is 1.0×10^{17} for TOAC^1-Alm and 1.2×10^{17} rad^{-2} s^{-2} for TOAC^8- and TOAC^{16}-Alm (24). These conversion factors are essentially the constant that relates the effective value of $\langle\omega^2(B)\rangle$ in the middle of the low-field region to the mean-square angular amplitude $\langle\alpha^2\rangle$ for isotropic libration (23). For comparison with Fig. 4 *a*, the values of $\langle\alpha^2\rangle\tau_c$ that are obtained by direct simulation are 2.2×10^{-11} and 3.2×10^{-11} rad^2 s for TOAC^1-Alm at 240 K and at 260 K, respectively; 1.4×10^{-11} rad^2 s for TOAC^8-Alm at 240 K; and 1.3×10^{-11} and 2.0×10^{-11} rad^2 s for TOAC^{16}-Alm at 240 K and at 260 K, respectively. It should be noted that the simulations at higher temperatures are less well determined than those at 200 K because of the lower echo intensities and the more limited number of echo delay times, τ, for which an echo may be observed (cf. the error bars on W_H in Fig. 3 *a*).

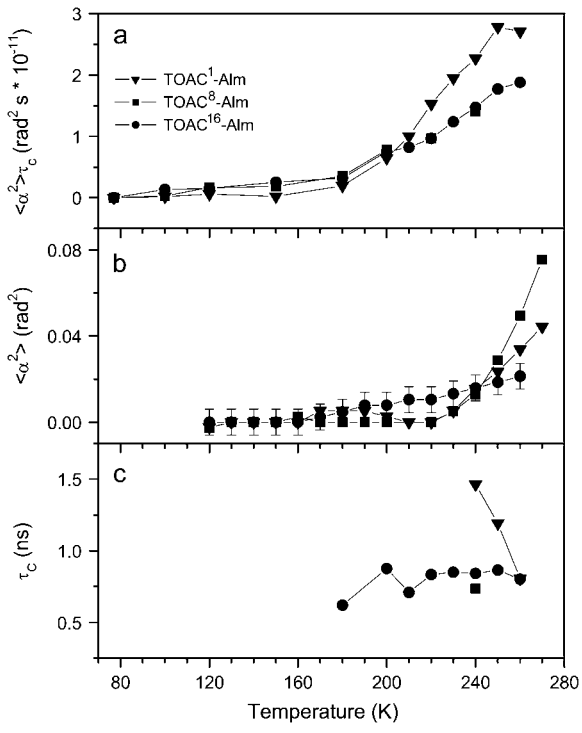

FIGURE 4 (*a*) Temperature dependence of the amplitude-correlation time product, $\langle\alpha^2\rangle\tau_c$, for TOAC^n-Alm ($n = 1$, 8, or 16) in DMPC bilayers. Values are obtained from measurements of the W_L relaxation rate parameter, together with the results of spectral simulations (see Fig. 1). (*b*) Temperature dependence of the librational amplitude, $\langle\alpha^2\rangle$, for TOAC^n-Alm ($n = 1$, 8, or 16) in DMPC bilayers. Values are obtained from the motionally averaged hyperfine splitting, $2\langle A_{zz}\rangle$, together with Eq. 5. (*c*) Temperature dependence of the librational correlation time, τ_c, for TOAC^n-Alm ($n = 1$, 8, or 16) in DMPC bilayers. Values are obtained from the amplitude-correlation product in *a* and the librational amplitude in *b*.

Fig. 4 *b* shows the temperature dependence of the mean-square amplitude, $\langle\alpha^2\rangle$, of the librational motion for the TOAC^n-Alm derivatives in DMPC bilayers. These values are derived from the motionally averaged hyperfine splittings according to Eq. 5 (34):

$$\langle A_{zz}\rangle = A_{zz} - (A_{zz} - A_{xx})\langle\alpha^2\rangle, \tag{5}$$

where the angular brackets indicate the motionally averaged hyperfine tensor (of principal elements A_{xx}, A_{yy}, and A_{zz}). For TOAC^1- and TOAC^8-Alm, the librational amplitude is almost vanishingly small up to 220 K and then increases relatively rapidly with increasing temperature. For TOAC^{16}-Alm, the librational amplitude is already measureable at 170 K but increases only slowly with increasing temperature. This is consistent with the extremely low relaxation rate and $\langle\alpha^2\rangle\tau_c$ product in the temperature range below 160 K (cf. Figs. 3 *a* and 4 *a*). The largest value of $\langle\alpha^2\rangle$ recorded in Fig. 4 *b* corresponds to a root mean-square amplitude of 16° (for TOAC^8-Alm at 270 K), which confirms that the small-amplitude approximation is appropriate at low temperatures.

Fig. 4 *c* shows the temperature dependence of the rotational correlation time, τ_c, for the librational motion of the TOAC^n-Alm derivatives in DMPC bilayers. Determinations of the amplitude-correlation time product, $\langle\alpha^2\rangle\tau_c$, from Fig. 4 *a* are combined with the amplitude (i.e., $\langle\alpha^2\rangle$) measurements that are given in Fig. 4 *b* to obtain these values for τ_c. Fig. 4 *c* thus represents the quotient of values from Fig. 4 *a* with those at the corresponding temperatures from Fig. 4 *b* for each of the three TOAC positions. For TOAC^{16}-Alm, the correlation time remains approximately constant at a value of ~0.8 ns up to 260 K. Evidently, torsional libration within the main body of the peptide backbone is not a strongly activated process. For TOAC^8-Alm, the correlation time for librational motion is similarly ~0.7 ns at 240 K but cannot be measured below this temperature because the torsional amplitude is too small. The effective correlation time of TOAC^1-Alm at 240 K is appreciably longer than those of TOAC^{16}-Alm and TOAC^8-

Alm at the same temperature but decreases rapidly to a value comparable to that of TOAC^{16} at 260 K. The librational correlation times found here for the spin-labeled peptide backbone in phospholipid membranes are longer than those for a spin-labeled lipid chain segment, which were determined to be in the region of 0.3 ns over the temperature range of 140–240 K (24).

DISCUSSION

In this work, we studied librational motions in the backbone of alamethicin when the peptide was bound to bilayer membranes of DMPC. Previous studies have shown that, in fluid-phase DMPC bilayers, the TOAC-labeled alamethicins adopt a transmembrane orientation and exhibit favorable hydrophobic matching with the lipid chains (8,9). For technical reasons, however, ED-EPR spectra can be recorded only at low temperatures, which correspond to the DMPC gel phase. Huang and co-workers (35) have found that alamethicin can adopt two different states when bound to lipid bilayer membranes: one in which the helix axis is oriented parallel to the membrane surface, and the other in which the helix orientation is transmembrane. The preferred state is determined by a critical peptide/lipid ratio that depends both on the particular lipid and on the temperature and degree of hydration (36–38). Whichever of the two orientations is adopted by alamethicin associated with gel-phase DMPC in these low-temperature measurements, it is likely that the helix backbone remains highly ordered, without large-amplitude angular fluctuations, and thus that the librational motions of the peptide backbone are comparable to those of alamethicin when it is fixed in a stable pore assembly.

The overall intensity of the librational fluctuations, as registered by the amplitude-correlation time product $\langle\alpha^2\rangle\tau_c$, is similar for the 8 and 16 positions of the TOAC residue in the alamethicin backbone but is larger for the N-terminal residue TOAC^1 (Fig. 4 *a*). Comparable values within the body of the peptide are to be expected for the torsional modes of the backbone. There are differences in angular amplitude (Fig. 4 *b*), which presumably reflect the structural differences at the various positions: TOAC^1 is situated at the N-terminus, adjacent to a proline residue, Pro^2; TOAC^8 is located toward the middle of the longer α-helical segment; and TOAC^{16} is situated beyond the bend in the region of Pro^{14} in the shorter C-terminal 3_{10}-helical segment. In consequence, the spin-labeled principal z axis is oriented differently relative to the molecular axis at the different positions of substitution: the inclination of the nitroxide principal axis to the longer helical segment of alamethicin is larger for TOAC^{16} than it is for TOAC^1 and TOAC^8 (8). Nevertheless, the librational correlation times all lie in the subnanosecond to nanosecond regime (Fig. 4 *c*) and are of comparable magnitude at 260 K. (Most likely, the large effective temperature dependence of τ_c for TOAC^1-Alm might be attributed to changes in orientation of this N-terminal residue.)

The amplitude-correlation time products, $\langle\alpha^2\rangle\tau_c$, that are determined in this work for the backbone torsions of alamethicin are of a similar size to those of previous studies on the torsional librations of phospholipid chains in bilayer membranes (22–24). The lipid chain librations are, however, significantly faster and the amplitudes are correspondingly larger than those of alamethicin (24). This correlation suggests that the torsional motions of the peptide backbone may be coupled to the librational fluctuations of the host lipid. In part, this coupling could be responsible for the lipid dependence of the properties of alamethicin channels (3,4,39).

The timescale of the librational fluctuations of the peptide backbone that are observed here is in a range that could influence the ion transport process. The internal pore radius for a regular polygonal arrangement of n transmembrane helices each with diameter $D \approx 1$ nm is (see, e.g., Marsh (40))

$$R_p = D[1/\sin(\pi/n) - 1]/2. \quad (6)$$

The conductance of such a pore of cross-sectional area $A = \pi R_p^2$ and length d, in a 1:1 electrolyte at concentration c_M, is given by (see, e.g., Hille (41))

$$g = 2c_M F(A/d)\langle u\rangle, \quad (7)$$

where $\langle u\rangle$ is the mean ionic mobility in the pore and F is the Faraday constant. The mean transit time for an ion in the pore is related to the mobility by

$$\langle t\rangle = d^2/(\langle u\rangle \Delta V), \quad (8)$$

where ΔV is the transmembrane potential. The first major channel state of alamethicin is characterized by a conductance of $g = 280$ pS in 1 M KCl (42). This may be identified with the oligomerization state $n = 6$ of alamethicin monomers (43). Thus, from Eqs. 6–8, the mean transit time for ions under a transmembrane potential of $\Delta V = 120$ mV is $\langle t\rangle \approx$ 14 ns, which is considerably longer than the correlation time for librational fluctuations of the alamethicin backbone.

Time-dependent fluctuations in polarizing electric fields that are associated with partial charges in the peptide backbone are, therefore, kinetically competent to participate in the movement of ions through the channel. It has been suggested that librational fluctuations in the peptide backbone of gramicidin may be involved directly in cation transport (18). In the latter case, the channel diameter is considerably smaller than that for alamethicin and the dehydrated ions are solvated directly by pore-lining groups of the peptide backbone. In the case of alamethicin, ions are transported through the aqueous pore and interactions with the peptide backbone take place via polarization of the pore-lining water molecules (43,44). Orientational fluctuations in the water dipoles that are driven by rapid torsional oscillations of the peptide backbone could hence be coupled to ion transport through the alamethicin channel. As in many other kinetic processes of biological relevance, rapid fluctuations coupled to the environment—in this case the lipid membrane—provide the driving force for slower, larger-scale transitions of a more

cooperative nature (45–47). Rapid fluctuations in electric polarization arising from peptide backbone librations are therefore suggested to drive the transitions that are involved in ion conduction within the alamethicin channel.

As in many cases of ionic conduction by hydrophobic peptides (see, e.g., Marsh (48)), the majority of alamethicin in the membrane is probably in an essentially monomeric state, although protochannel formation is indicated by the observation of instantaneous diffusion, which arises from spin-spin interactions between monomers. As mentioned above, the relatively rigid ordering of the peptide associated with gel-phase lipid is likely to be similar to, and is taken here as a model for, the peptide assembled in channel aggregates—at least for the backbone librational motions. It should also be noted that ion conduction has been observed with alamethicin when the lipid chains of the membrane are in an ordered gel state (3). Finally, the methodology developed here to study backbone fluctuations in alamethicin can be applied directly also to systems in which the peptides are preassembled, e.g., in covalently linked transmembrane helices.

D.M. and colleagues in Calabria are members of the Cooperation in the field of Scientific and Technical Research (COST) P15 Action of the European Union.

M.D.Z. and C.T. are grateful to the Ministry of Education, Universities, and Research (Italy) for financial support through the Programmi di Rilevante Interesse Nazionale (PRNI) 2006 grant.

REFERENCES

1. Fox, R. O. Jr., and F. M. Richards. 1982. A voltage-gated ion channel model inferred from the crystal structure of alamethicin at 1.5 Å resolution. *Nature.* 300:325–330.
2. Opsahl, L. R., and W. W. Webb. 1994. Transduction of membrane tension by the ion-channel alamethicin. *Biophys. J.* 66:71–74.
3. Boheim, G., W. Hanke, and H. Eibl. 1980. Lipid phase transition in planar bilayer membrane and its effect on carrier- and pore-mediated ion transport. *Proc. Natl. Acad. Sci. USA.* 77:3403–3407.
4. Hall, J. E., I. Vodyanoy, T. M. Balasubramanian, and G. R. Marshall. 1984. Alamethicin—a rich model for channel behavior. *Biophys. J.* 45:233–247.
5. Keller, S. L., S. M. Bezrukov, S. M. Gruner, M. W. Tate, I. Vodyanoy, and V. A. Parsegian. 1993. Probability of alamethicin conductance states varies with nonlamellar tendency of bilayer phospholipids. *Biophys. J.* 65:23–27.
6. Archer, S. J., J. F. Ellena, and D. S. Cafiso. 1991. Dynamics and aggregation of the peptide ion channel alamethicin. *Biophys. J.* 60: 389–398.
7. Barranger-Mathys, M., and D. S. Cafiso. 1994. Collisions between helical peptides in membranes monitored using electron paramagnetic resonance: evidence that alamethicin is monomeric in the absence of a membrane potential. *Biophys. J.* 67:172–176.
8. Marsh, D., M. Jost, C. Peggion, and C. Toniolo. 2007. TOAC spin labels in the backbone of alamethicin: EPR studies in lipid membranes. *Biophys. J.* 92:473–481.
9. Marsh, D., M. Jost, C. Peggion, and C. Toniolo. 2007. Lipid chainlength dependence for incorporation of alamethicin in membranes: EPR studies on TOAC-spin labelled analogues. *Biophys. J.* 92:4002–4011.
10. Boheim, G., and H.-A. Kolb. 1978. Analysis of the multi-pore system of alamethicin in a lipid membrane. I. Voltage-jump current-relaxation measurements. *J. Membr. Biol.* 38:99–150.
11. Nakaie, C. R., S. Schreier, and A. C. M. Paiva. 1983. Synthesis and properties of spin-labeled angiotensin derivatives. *Biochim. Biophys. Acta.* 742:63–71.
12. Marchetto, R., S. Schreier, and C. R. Nakaie. 1993. A novel spin-labeled amino acid derivative for use in peptide synthesis—(9-fluorenylmethyloxycarbonyl)-2,2,6,6-tetramethylpiperidine-*N*-oxyl-4-amino-4-carboxylic acid. *J. Am. Chem. Soc.* 115:11042–11043.
13. Monaco, V., F. Formaggio, M. Crisma, C. Toniolo, P. Hanson, and G. L. Millhauser. 1999. Orientation and immersion depth of a helical lipopeptaibol in membranes using TOAC as an ESR probe. *Biopolymers.* 50:239–253.
14. Karim, C. B., T. L. Kirby, Z. Zhang, Y. Nesmelov, and D. D. Thomas. 2004. Phospholamban structural dynamics in lipid bilayers probed by a spin label rigidly coupled to the peptide backbone. *Proc. Natl. Acad. Sci. USA.* 101:14437–14442.
15. Marsh, D., M. Jost, C. Peggion, and C. Toniolo. 2007. Solvent dependence of the rotational diffusion of TOAC-spin-labelled alamethicin. *Chem. Biodivers.* 4:1269–1274.
16. Marsh, D., and C. Toniolo. 2008. Polarity dependence of EPR parameters for TOAC and MTSSL spin labels: correlation with DOXYL spin labels for membrane studies. *J. Magn. Reson.* 190:211–221.
17. Crisma, M., C. Peggion, C. Baldini, E. J. MacLean, N. Vedovato, G. Rispoli, and C. Toniolo. 2007. Crystal structure of a spin-labelled, channel-forming, alamethicin analogue. *Angew. Chem. Int. Ed.* 46:2047–2050.
18. North, C. L., and T. A. Cross. 1995. Correlations between function and dynamics: time scale coincidence for ion translocation and molecular dynamics in the gramicidin channel backbone. *Biochemistry.* 34:5883–5895.
19. Domene, C., A. Grottesi, and M. S. Sansom. 2004. Filter flexibility and distortion in a bacterial inward rectifier K^+ channel: simulation studies of KirBac1.1. *Biophys. J.* 87:256–267.
20. Grottesi, A., C. Domene, B. Hall, and M. S. Sansom. 2005. Conformational dynamics of M2 helices in KirBac channels: helix flexibility in relation to gating via molecular dynamics simulations. *Biochemistry.* 44:14586–14594.
21. Bartucci, R., D. A. Erilov, R. Guzzi, L. Sportelli, S. A. Dzuba, and D. Marsh. 2006. Time-resolved electron spin resonance studies of spin-labelled lipids in membranes. *Chem. Phys. Lipids.* 141:142–157.
22. Bartucci, R., R. Guzzi, D. Marsh, and L. Sportelli. 2003. Chain dynamics in the low-temperature phases of lipid membranes by electron spin-echo spectroscopy. *J. Magn. Reson.* 162:371–379.
23. Erilov, D. A., R. Bartucci, R. Guzzi, D. Marsh, S. A. Dzuba, and L. Sportelli. 2004. Echo-detected electron paramagnetic resonance spectra of spin-labeled lipids in membrane model systems. *J. Phys. Chem. B.* 108:4501–4507.
24. Erilov, D. A., R. Bartucci, R. Guzzi, D. Marsh, S. A. Dzuba, and L. Sportelli. 2004. Librational motion of spin-labeled lipids in high-cholesterol containing membranes from echo-detected EPR spectra. *Biophys. J.* 87:3873–3881.
25. De Simone, F., R. Guzzi, L. Sportelli, D. Marsh, and R. Bartucci. 2007. Electron spin-echo studies of spin-labelled lipid membranes and free fatty acids interacting with human serum albumin. *Biochim. Biophys. Acta.* 1768:1541–1549.
26. Peggion, C., M. Jost, C. Baldini, F. Formaggio, and C. Toniolo. 2007. Total synthesis in solution of TOAC-labelled alamethicin F50/5 analogues. *Chem. Biodivers.* 4:1183–1199.
27. Peggion, C., I. Coin, and C. Toniolo. 2004. Total synthesis in solution of alamethicin F50/5 by an easily tunable segment condensation approach. *Biopolymers.* 76:485–493.
28. Peggion, C., M. Jost, W. M. de Borggraeve, M. Crisma, F. Formaggio, and C. Toniolo. 2007. Conformational analysis of TOAC-labelled alamethicin F50/5 analogues. *Chem. Biodivers.* 4:1256–1268.
29. Dzuba, S. A., Yu. D. Tsvetkov, and A. G. Maryasov. 1992. Echo-detected EPR spectra of nitroxides in organic glasses: model of orientational molecular motions near equilibrium position. *Chem. Phys. Lett.* 188:217–222.

30. Salikov, K. M., and Y. D. Tsvetkov. 1979. Electron spin-echo studies of spin-spin interactions in solids. *In* Time Domain Electron Spin Resonance. L. Kevan and R. N. Schwartz, editors. Wiley-Interscience, New York. 231–278.

31. Marsh, D. 2006. Orientation of TOAC amino-acid spin labels in α-helices and β-strands. *J. Magn. Reson.* 180:305–310.

32. Tabak, M., A. Alonso, and O. R. Nascimento. 1983. Single crystal ESR studies of a nitroxide spin label. I. Determination of the *G* and *A* tensors. *J. Chem. Phys.* 79:1176–1184.

33. Dzuba, S. A. 1996. Librational motion of guest spin probe molecules in glassy media. *Phys. Lett. A.* 213:77–84.

34. Van, S. P., G. B. Birrell, and O. H. Griffith. 1974. Rapid anisotropic motion of spin labels. Models for motion averaging of the ESR parameters. *J. Magn. Reson.* 15:444–459.

35. Huang, H. W. 2006. Molecular mechanism of antimicrobial peptides: the origin of cooperativity. *Biochim. Biophys. Acta.* 1758:1292–1302.

36. Heller, W. T., K. He, S. J. Ludtke, T. A. Harroun, and H. W. Huang. 1997. Effect of changing the size of lipid headgroup on peptide insertion into membranes. *Biophys. J.* 73:239–244.

37. Chen, F. Y., M. T. Lee, and H. W. Huang. 2002. Sigmoidal concentration dependence of antimicrobial peptide activities: a case study on alamethicin. *Biophys. J.* 82:908–914.

38. Lee, M. T., W. C. Hung, F. Y. Chen, and H. W. Huang. 2005. Many-body effect of antimicrobial peptides: on the correlation between lipid's spontaneous curvature and pore formation. *Biophys. J.* 89:4006–4016.

39. Bezrukov, S. M., R. P. Rand, I. Vodyanoy, and V. A. Parsegian. 1998. Lipid packing stress and polypeptide aggregation: alamethicin channel probed by proton titration of lipid charge. *Faraday Discuss.* 111:173–183.

40. Marsh, D. 1999. Spin label ESR spectroscopy and FTIR spectroscopy for structural/dynamic measurements on ion channels. *Methods Enzymol.* 294:59–92.

41. Hille, B. 1992. Ionic Channels of Excitable Membranes. Sinauer Associates, Sunderland, MA.

42. Hanke, W., and G. Boheim. 1980. The lowest conductance state of the alamethicin pore. *Biochim. Biophys. Acta.* 596:456–462.

43. Breed, J., P. C. Biggin, I. D. Kerr, O. S. Smart, and M. S. Sansom. 1997. Alamethicin channels—modelling via restrained molecular dynamics simulations. *Biochim. Biophys. Acta.* 1325:235–249.

44. Tielemann, D. P., J. Breed, H. J. C. Berendsen, and M. S. P. Sansom. 1999. Alamethicin channels in a membrane: molecular dynamics simulations. *Faraday Discuss.* 111:209–223.

45. Beece, D., L. Eisenstein, H. Frauenfelder, D. Good, M. C. Marden, L. Reinisch, A. H. Reynolds, L. B. Sørensen, and K. T. Yue. 1980. Solvent viscosity and protein dynamics. *Biochemistry.* 19:5147–5157.

46. Welch, G. R., B. Somogyi, and S. Damjanovich. 1982. The role of protein fluctuations in enzyme action: a review. *Prog. Biophys. Mol. Biol.* 39:109–146.

47. Damjanovich, S., B. Somogyi, and G. R. Welch. 1983. Protein fluctuation and enzyme activity. *J. Theor. Biol.* 105:25–33.

48. Marsh, D. 1996. Peptide models for membrane channels. *Biochem. J.* 315:345–361.